ISSN 1392–1207. MECHANIKA. 2016 Volume 22(4): 318–322

Acoustic nonlinearity of the planar slip in the Cu-Zn alloy subjected to low-cycle fatigue

C. S. Kim
Chosun University, 309, Pilmun-daero, Dong-gu, Geangju, 501-759 Korea, E-mail: chs2865@chosun.ac.kr

crossref http://dx.doi.org/10.5755/j01.mech.22.4.16165

1. Introduction

Higher harmonics of acoustic waves are physically related to the nonlinearity of materials in interatomic relations. The nonlinear stress-strain relation in solid media can be expressed by second order elastic constants and nonlinear coefficients. Acoustic nonlinearity is highly sensitive to microstructural parameters. When a single and fundamental ultrasonic wave frequency propagates into a solid medium, the ultrasonic waveform responds to the stress-strain relation and is distorted due to wave dispersion that is dependent on the amplitude. If the displacement of an ultrasonic wave with a finite amplitude is high enough and is introduced to a solid medium, it gives rise to plastic modification, and the output signal waveform propagating through the material may be distorted. Thus, high-order harmonics of an incident ultrasonic wave may be generated by the nonlinear interactions [1-5].

Structural materials under fatigue loading conditions are generally vulnerable to fatigue failure at even below the yield strength. In the initial stage of fatigue damage (crack initiation stage), micromechanical properties of materials can vary with respect to vacancy, dislocation, twin, stacking fault, and grain structure. Changes in the mechanical properties of structural materials are more closely related to microstructural evolutions influenced by dislocations and their configurations. Slip becomes localized and leads to a persistent slip band (PSB). These PSBs serve as stress concentrators under cyclic loading condition and generate microcracks leading to catastrophic failure of the mechanical materials. Therefore, in addition to the destructive characterization, advanced nondestructive evaluation techniques for damage monitoring without damaging the structures would be indispensable but challenging [6-10].

In the present, acoustic nonlinearity has been investigated in many research areas, such as physics, mechanics and materials, for the characterization of micromechanical properties [11-13]. However, there is little report on the acoustic nonlinearity of planar slip materials. In this study, we experimentally investigate the acoustic nonlinearity of a planar-array slip material and examine the influence of dislocations on acoustic nonlinearity.

2. Experimental procedure

The planar-array slip material Cu-Zn alloy was used. Test materials were prepared to have a gauge length of 15 mm and were heat-treated at 600°C. The average grain size was measured by the linear intercept method. The test specimens were carefully prepared by chemical polishing after mechanical polishing to remove the damaged layer from the process of mechanical cutting. A cyclic loading test was conducted under strain amplitude control at room temperature to change the dislocation substructure using predetermined fatigue cycles. A triangular waveform was applied to give a constant strain rate of $6 \times 10^{-4}s^{-1}$. The failure cycles were determined when the saturation stress decreased to 20%.

Physically, if an ultrasonic wave having a sufficient amplitude and given frequency is introduced into a nonlinear medium, the fundamental waveform is distorted as it propagates due to the velocity variation, which is dependent on the wave amplitude; thus, harmonic components of the fundamental wave are generated.

Fig. 1 shows a schematic figure of acoustic nonlinearity showing the input signal and output signal. The incident ultrasonic waveform is distorted by the quadratic nonlinearity of nonlinear materials, and harmonic waves are generated. The superharmonic generation method was applied to measure the acoustic nonlinearity [14, 15]. The acoustic nonlinearity system (RAM5000 SNAP) consisted of a high power attenuator (RA-31), a high power 50 Ω terminator (RL-50), and a high power 6 dB attenuator (RA-6), as schematically shown in Fig. 2. A piezoelectric probe with a fundamental frequency of 10 MHz was placed on one side of the specimen as a transmitter, and a wide band-width probe with a frequency of 20 MHz was attached on the other side of the specimen as a receiver to obtain second-order harmonic waves.

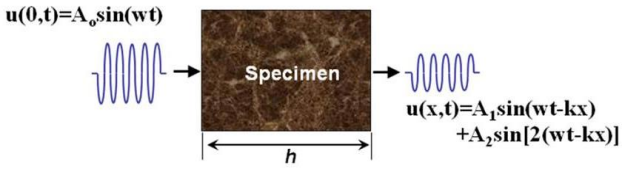

Fig. 1 Schematic figure of input and output waves showing superharmonic generation

The nonlinearity parameter (β) was determined by the amplitude ratio between the initially pure wave and the second-order harmonic [16, 17]. The amplitudes, i.e., A_1 of the initially pure wave and A_2 of the second-order harmonic, were digitized. The absolute parameter β was physically expressed with respect to the particle displacement. However, the relative value of acoustic nonlinearity is more useful than the absolute value for characterizing damage accumulation because the received waveform contains system nonlinearity from the wedges, measuring components, and specimens. For that reason, the ratio of acoustic nonlinearity (β/β_0), i.e., β divided by the nonlinearity parameter of intact specimen (β_0), was used to neglect the nonlinearity of the measurement system. In addition, the particle displacement

amplitude has linear relations with the magnitudes of fast Fourier transform (FFT) F_1 and F_2. The acoustic nonlinearity parameter in this study was simply determined by $\beta' = \left(F_2 / F_1^2\right) 1/h$, where F_1 and F_2 represent the amplitudes of the harmonic waves and h is the thickness of the test specimen.

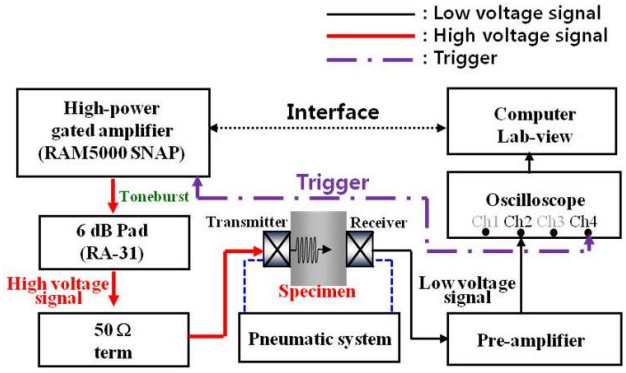

Fig. 2 Schematic diagram of the acoustic nonlinearity system and signal flow

The test materials were mechanically machined into a rectangular shape (15 mm long, 10 mm wide, and 10 mm thick). For the microstructural observation, the fatigue-tested specimens were cut normal to the loading direction. The surface microstructure was observed using optical microscopy after chemical etching in a solution of 25 ml NH_4OH and 50 ml H_2O_2 (3%). Thin foils were carefully prepared by the electrolytic polishing method. The electrolytic solution was prepared with 165 ml of NHO_3 and 335 ml of CHO_4. Dislocation substructures of the foils were investigated by transmission electron microscopy (TEM).

3. Results and discussion

The cyclic hardening curves of the planar-array slip material Cu-Zn alloy under total strain amplitudes are shown in Fig. 3, a. The test materials exhibited cyclic hardening after several tens of cycles and then became saturated. The strain hardening was observed to be most pronounced during the early fatigue cycles, where after the strain hardening became saturated. The fatigue life curve of Cu-Zn alloy is shown in Fig. 3, b. A power law equation that follows the Manson-Coffin law can be well fitted to the experimental data [18]. The fatigue ductility coefficient and fatigue ductility exponent were 0.18 and -0.56, respectively.

$$\varepsilon_{ap} = \varepsilon_f^{'} \left(2N_f\right)^c, \quad (1)$$

where ε_{ap} is the plastic strain, $\varepsilon_f^{'}$ is the fatigue ductility coefficient, N_f is number of cycles to failure, and c the fatigue ductility exponent.

Fig. 4 shows the acoustic nonlinearity of the Cu-Zn alloy under total strain amplitudes. The typical power spectrum of the as-annealed sample at 600°C is shown in Fig. 4, a. The fundamental frequency amplitude (A_1) does not change during fatigue damage, but the second-order harmonic (A_2) signal may be changed due to the material nonlinearity.

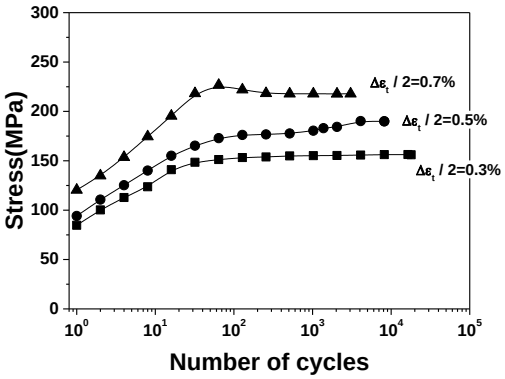

a

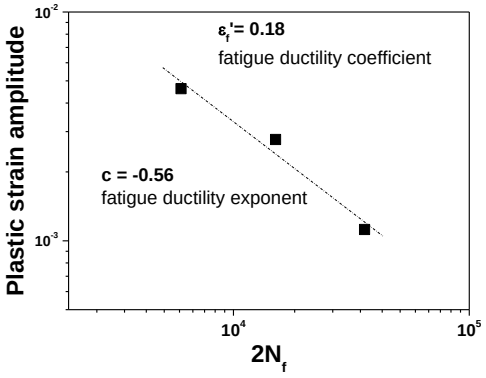

b

Fig. 3 Low-cycle fatigue of the Cu-Zn alloy under total strain amplitudes: a - variation of the cyclic stresses with the number of cycles; b - fatigue ductility coefficient and ductility exponent of the Cu-Zn alloy

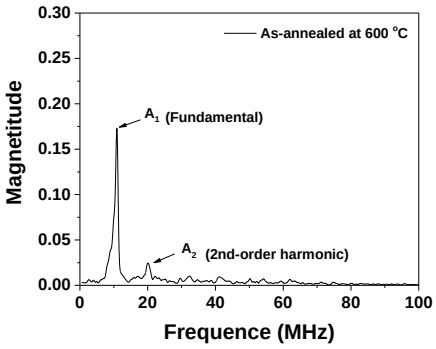

a

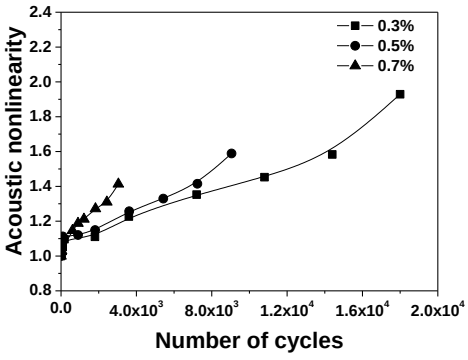

b

Fig. 4 Acoustic nonlinearity of the Cu-Zn alloy: a - typical FFT data of the as-annealed sample at 600°C; b - variation of the acoustic nonlinearity with the number of cycles and total stain amplitude

The nonlinearity parameter increased with cyclic loading due to micromechanical deformation as depicted in Fig. 4, b. It clearly shows the fundamental and second-order harmonics in the voltage signal based on the FFT. It can be noted that there is no saturation region of acoustic nonlinearity with the number of cycles.

In general, the higher harmonics are generated by the distortion of the acoustic waveform during propagation in nonlinear elastic materials. This is closely related to the nonlinearity involving defects, microstructural features, and disruptions in the lattice structure of the materials. In addition, micro-strains in materials evolving from second particles and dislocations may influence the distortion of acoustic waves. In metallic materials, misfit dislocations give rise to a locally varying strain field around the dislocations. They also generate dislocation displacements and affect the nonlinear stress-strain relation. In a solid that contains dislocations capable of glide displacements via small shear stresses, these dislocation displacements also affect the nonlinear stress-strain relation. Hikata et al. conducted numerical and experimental investigations of the dislocation contribution to the generation of second harmonic ultrasonic waves in a pure aluminum single crystal [19]. They showed in the model that the amplitude of the second harmonic wave was dependent on the dislocation displacement as follows:

$$A_2 \propto \frac{12}{5}\frac{\Omega \Lambda E^2 L^4 R^3}{\mu^3 b^2}\sigma, \qquad (2)$$

where Ω is the conversion factor from shear strain to longitudinal strain, Λ is the dislocation density, E is the second order elastic modulus, L is the dislocation loop length, R is the resolving shear factor, μ is the shear stress, and σ is the static stress.

This indicated that the second harmonic wave influenced the dislocation displacement related to the dislocation density, as well as the loop length. In this study, the dominant microstructural development during fatigue of the Cu-Zn alloy was dislocation evolution, such as dislocation density, loop length, and substructures. In the initial fatigue deformation, acoustic nonlinearity increased rapidly as shown in Fig. 4(b), was monotonous under medium fatigue, and finally increased quickly again. In order to understand the microstructural features influencing the wave distortion of the acoustic wave resulting in superharmonic generation, the microstructural evolution during fatigue damage was examined and then the variation was interpreted in the acoustic nonlinearity.

Figs. 5, a-c depict the variations in the dislocation substructures of the planar-array slip material Cu-Zn alloy with different fatigue cycles. The dislocation substructures of face-centered-cubic materials depends strongly on the strain, stacking fault, and temperature [20]. Cu-Zn alloys are typical planar-array slip materials with a low stacking fault energy, where cross slip does not happen easily due to the low stacking fault energy [21]. In the present study, a planar-array dislocation substructure was developed and clearly observed. These results corresponded well to previously reported results by other researchers [20, 21]. Figs. 5, d-f represent the image quality (IQ) maps of the Cu-Zn alloy under a strain amplitude of 0.3%. The IQ describes the quality of an electron backscatter diffraction depending on the material and its condition. The IQ factor of diffraction patterns is influenced by the perfection of the crystal lattice. Therefore, lattice distortions of the crystalline structure within the diffraction volume will produce a

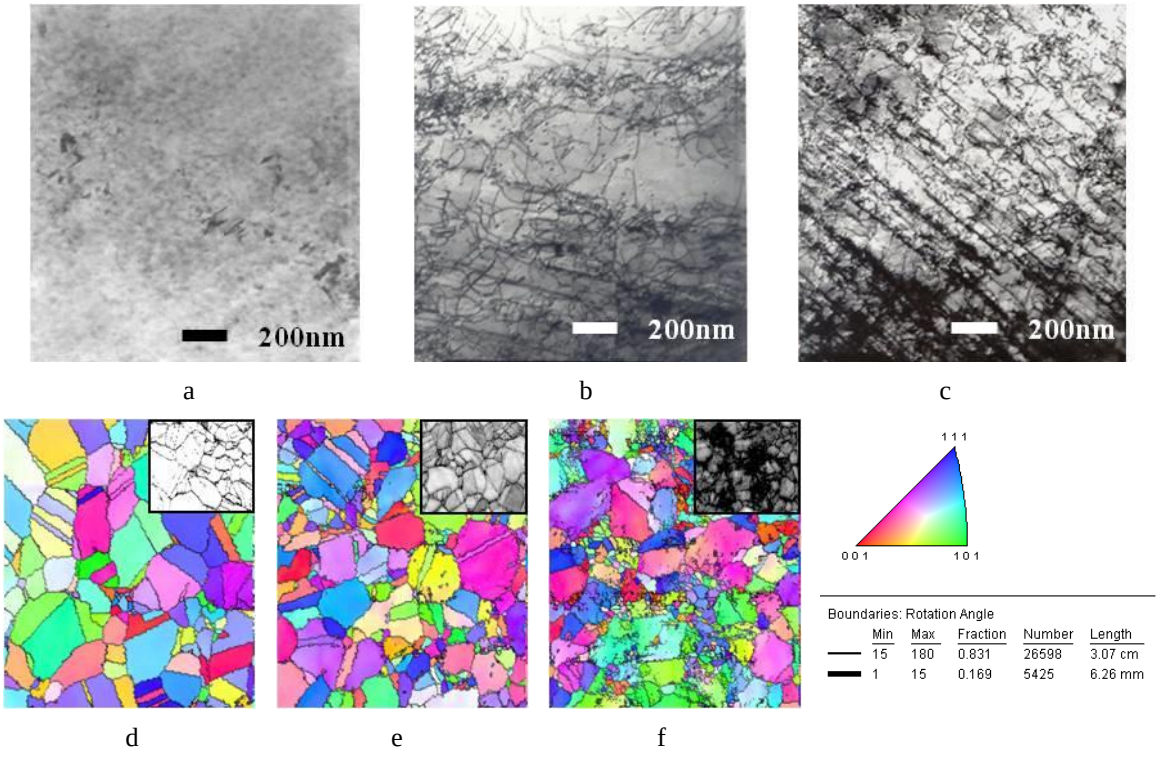

Fig. 5 TEM and EBSD micrographs showing the planar dislocation substructure of the Cu-Zn alloy under a strain amplitude of 0.3%: a,d - 0 cycle (as-annealed); b,e - 3600 cycles ($0.2N_f$); c,f - 14400 cycles ($0.8N_f$)

lower IQ. As the fatigue life increased, the darker gray shades in the images continuously increased, indicating the stain distribution of the Cu-Zn alloy. In the present study, the dominant microstructural evolution during the fatigue of the planar-array slip material Cu-Zn alloy varied in the dislocation substructure, such as the dislocation density, loop length, and dislocation configurations. The loop length of dislocations may change depending on the condition of dislocation pinning, i.e., the loop length may either increase or decrease. The dislocation density may increase during plastic deformation with several orders of magnitude higher than the annealed state. Therefore, the variation in the dislocation density could be a dominant factor influencing the acoustic nonlinearity of the planar-array slip material Cu-Zn alloy during fatigue damages.

In general, micromechanical properties are often observed due to the development of dislocations, slip bands, and dislocation substructures when the materials accumulate fatigue damage. These strain fields caused by misfit dislocations are enough to distort the crystal lattice and vary the phase velocity of the acoustic waves depending on the amplitude. In addition to the dislocation, grain deformation, such as slips and mechanical twins, could be factors leading to wave distortion during propagation through solid materials. The presented ultrasonic nonlinearity measurement can evaluate the dislocation evolution of planar-slip materials subjected to low-cycle fatigues and has the potential to characterize damages and predict the fatigue life of metallic materials. For practical applications, however, a more extensive and quantitative examination is necessary.

4. Conclusions

The acoustic nonlinearity increased with the fatigue cycle due to plastic deformation. The increase of dislocation density was clearly observed during fatigue testing of the planar-array slip material Cu-Zn alloy via electron microscopy and electron backscattered diffraction techniques. In this work, it was found that the low-cycle fatigue damage was enough to cause noticeable variations in the acoustic nonlinearity. It could be noted that there was no saturation region of acoustic nonlinearity with the number of cycles. Consequently, acoustic nonlinearity could be a potential index to characterize cyclic deformation with respect to dislocation substructures. Additionally, it has the potential to characterize damages and predict the fatigue life of metallic materials.

Acknowledgements

This work was supported by the National Research Foundation of Korea (NRF) grant funded by the Korean government MSIP (No.2008-0062283).

References

1. **Xing, Y.; Jhu, W.; Liu, C.J.; Xuan, F.Z.; Wang, Y.N.; Kuang, W.C.** 2015. Creep degradation characterization of titanium alloy using nonlinear ultrasonic technique, NDT & E Int. 72: 41-49. http://dx.doi.org/10.1016/j.ndteint.2015.02.001.
2. **Kim, C.S.** 2012. Acoustic nonlinearity of narrowband laser-generated surface wave in plastic deformed aluminum alloy, Chinses Phys. Lett. 29(12): 120701. http://dx.doi.org/10.1088/0256-307X/29/12/120701.
3. **Van Den Abeele, K.E.A.; Johnson, P.A.; Sutin, A.** 2000. Nonlinear elastic wave spectroscopy(NEWS) techniques to discern material damage, part 1: nonlinear wave modulation spectroscopy (NWMS), Res. Nondestr. Eval. 12: 17-30. http://dx.doi.org/10.1080/09349840009409646.
4. **Liu, M.; Tang, G.; Jacobs, L.J.; Qu, J.** 2012. Measuring acoustic nonlinearity parameter using collinear wave mixing, J. Appl. Phys. 112: 024908. http://dx.doi.org/10.1063/1.4739746.
5. **Jacob, X.; Catheline, S.; Gennisson, J.L.; Barriere, C.** 2007. Nonlinear shear wave interaction in soft solids, J. Acoust. Soc. Am. 122(4): 1917-1926. http://dx.doi.org/10.1121/1.2775871.
6. **Robert, E.G.Jr.** 2004. Non-contact ultrasonic techniques, Ultrasonics. 42: 9-16. http://dx.doi.org/10.1016/j.ultras.2004.01.101.
7. **Park, J.S.; Kim, M.S.; Chi, B.H.; Jang, C.H.** 2013. Correlation of metallurgical analysis & higher harmonic ultrasonic response for long term isothermally aged and crept FM steel for USC TPP turbine rotors, NDT&E Int. 54: 159-165. http://dx.doi.org/10.1016/j.ndteint.2012.10.008.
8. **Ruiz, A.; Ortiz, N.; Kim, J.Y.; Jacobs, L.J.** 2013. Application of ultrasonic methods for early detection of thermal damage in 2205 duplex stainless steel, NDT&E Int. 54: 19-26. http://dx.doi.org/10.1016/j.ndteint.2012.11.009.
9. **Ohtani, T.; Ogi, H.; Hirao, M.** 2006. Electromagnetic acoustic resonance to assess creep damage in Cr-Mo-V steel, Japan Soc. Appl. Phys. 45(5B): 4526-4533. http://dx.doi.org/10.1143/JJAP.45.4526.
10. **Raj, B.; Choudhary, B.K.; Singh Raman, P.K.** 2004. Mechanical properties and non-destructive evaluation of chrominum-molybdenum ferritic steels for steam generator application, Int. J. Pres. Ves. Pip. 81: 521-534. http://dx.doi.org/10.1016/j.ijpvp.2003.12.010.
11. **Jhang, K.Y.** 2009. Nonlinear ultrasonic techniques for nondestructive assessment of micro damage in material: A review, Inter. J. Precis. Eng. Man. 10: 123-135. http://dx.doi.org/10.1007/s12541-009-0019-y.
12. **Herrmann, J.; Kim, J.Y.; Jacobs, L.J.; Qu, J.; Littles, J.W.; Savage, M.F.** 2006. Assessment of material damage in a nickel-base superalloy using nonlinear Rayleigh surface waves, J. Appl. Phys. 99: 24913. http://dx.doi.org/10.1063/1.2204807.
13. **Xiang, Y.; Deng, M.; Xuan, F.Z.; Liu, C.J.** 2011. Cumulative second-harmonic analysis of ultrasonic Lamb waves for ageing behavior study of modified-HP austenite steel, Ultrasonics 51: 974-981. http://dx.doi.org/10.1016/j.ultras.2011.05.013.
14. **Xiang, Y.X.; Deng, M.X.; Xuan, F.Z.; Chen, H.; Chen, D.Y.** 2012. Creep damage evaluation of titanium alloy using nonlinear ultrasonic Lamb waves, Chin. Phys. Lett. 29(10): 106202. http://dx.doi.org/10.1088/0256-307X/29/10/106202.
15. **Kumar, A.; Torbet, C.J.; Pollock, T.M.; Jones, J.W.** 2010. In situ characterization of fatigue damage evolution in a cast Al alloy via nonlinear ultrasonic measurements, Acta Mater. 58: 2143-2154. http://dx.doi.org/10.1016/j.actamat.2009.11.055.
16. **Viswanath, A.; Rao, B.P.C.; Mahadevan, S.; Jaya-**

kumar, T.; Raj, B. 2010. Microstructural characterization of M250 grade maraging steel using nonlinear ultrasonic technique, J. Mater. Sci. 45: 6719-6726. http://dx.doi.org/10.1007/s10853-010-4765-0.
17. **Balasubramaniam, K.; Valluri, J.S.; Prakash, R.V.** 2011. Creep damage characterization using a low amplitude nonlinear ultrasonic technique, Mater. Character. 62(3): 275-286. http://dx.doi.org/10.1016/j.matchar.2010.11.007.
18. **Hertzber, R.W.** 1976. Deformation and Fracture Mechanics of Engineering Materials, John Wiley & Son. Inc., NJ, 415p.
19. **Hikata, A.; Chick B.B.; Elbaum, C.** 1965. Dislocation contribution to the second harmonic generation of ultrasonic wave, J. Appl. Phys. 36: 229-236. http://dx.doi.org/10.1063/1.1713881.
20. **Madhoun, Y.; Mohamed, A.; Bassim, M.N.** 2003. Cyclic stress–strain response and dislocation structures in polycrystalline aluminum, Mater. Sci. Eng. A. 359: 220-227. http://dx.doi.org/10.1016/S0921-5093(03)00347-2.
21. **Feltner, C.E.; Laird, C.** 1967. Cyclic stress-strain response of F.C.C. metals and alloys—II Dislocation structures and mechanisms, Acta Metall. 15: 1633-1653. http://dx.doi.org/10.1016/0001-6160(67)90138-1.

C. S. Kim

ACOUSTIC NONLINEARITY OF THE PLANAR SLIP IN THE Cu-Zn ALLOY SUBJECTED TO LOW-CYCLE FATIGUE

S u m m a r y

The objective of this study is to investigate experimentally the cyclic deformation in a planar slip material using acoustic nonlinearity. Observation and characterization of the dislocation substructure are conducted using an electron microscope. The acoustic nonlinearity was obtained by a superharmonic generation technique for different levels of fatigue-damaged specimens. The microstructural effects on nonlinearity are discussed in terms of the extent of planar-array dislocations in the substructures after the low-cycle fatigue. The acoustic nonlinearity of Cu-Zn alloy increased with the number of fatigue cycles due to the evolution of dislocation substructures. Consequently, acoustic nonlinearity could be a potential index to characterize cyclic deformation with respect to dislocation substructures.

Keywords: acoustic nonlinearity, dislocation, harmonic generation, fatigue.

Received February 04, 2016
Accepted July 04, 2016